

FED LIBRARY JAN 29 1982

*cy. 22*

# 60 GHz GYROTRON DEVELOPMENT PROGRAM

**Quarterly Report No. 7  
January through March 1981**

**J.F. Shively, S.J. Evers, S.J. Evans, and D.S. Stone**

FUSION ENERGY DIVISION LIBRARY

**Report prepared by:  
Varian Associates, Inc.  
Palo Alto Microwave Tube Division  
611 Hansen Way  
Palo Alto, California 94303**

**Purchase Order Subcontract No. 53Y-21453C**

**For  
Oak Ridge National Laboratory  
Oak Ridge, Tennessee 37830**

**Operated By:  
UNION CARBIDE CORPORATION  
for the  
U.S. Department Of Energy**

**Contract No. W-7405-eng-26**



3 4456 0536806 3

**Printed in the United States of America. Available from:  
National Technical Information Service  
U.S. Department of Commerce  
5255 Port Royal Road, Springfield, Virginia 22161  
NTIS price codes — Printed Copy: A03 Microfiche A01**

This report was prepared as an account of work sponsored by an agency of the United States Government. Neither the United States Government nor any agency thereof, nor any of their employees, makes any warranty, express or implied, or assumes any legal liability or responsibility for the accuracy, completeness, or usefulness of any information, apparatus, product, or process disclosed, or represents that its use would not infringe privately owned rights. Reference herein to any specific commercial product, process, or service by trade name, trademark, manufacturer, or otherwise, does not necessarily constitute or imply its endorsement, recommendation, or favoring by the United States Government or any agency thereof. The views and opinions of authors expressed herein do not necessarily state or reflect those of the United States Government or any agency thereof.

60 GHz GYROTRON DEVELOPMENT PROGRAM

Quarterly Report No. 7  
January through March 1981

J.F. Shively, S.J. Evers, S.J. Evans and D.S. Stone

Report prepared by  
Varian Associates, Inc.  
Palo Alto Microwave Tube Division  
611 Hansen Way  
Palo Alto, California 94303

For:  
Oak Ridge National Laboratory  
Oak Ridge, Tennessee 37830

Operated by  
UNION CARBIDE CORPORATION

for the  
U.S. Department of Energy

Contract No. W-7405-eng-26

## ABSTRACT

The objective of this program is to develop a microwave oscillator capable of producing 200 kW of CW power at 60 GHz. The use of cyclotron resonance interaction is being pursued.

The design, early construction, and test phases are discussed. A peak output power of over 200 kw was obtained with over 50% efficiency at pulse durations of 20  $\mu$ s.

## TABLE OF CONTENTS

<u>Section</u>		<u>Page</u>
I.	INTRODUCTION .....	1
II.	GYROTRON BEHAVIOR STUDY .....	3
	A. Arcing and Crowbar Investigation .....	3
	B. New Cathode Material .....	6
	C. RF Behavior .....	6
	D. Cavity and Output Taper Design .....	9
III.	SUPERCONDUCTING SOLENOID MAGNET .....	13
IV.	COLLECTOR .....	14
V.	CW WINDOW DESIGNS .....	15
	A. Location of Passbands .....	15
	B. Bandwidth .....	15
	C. Dielectric Loss .....	19
	D. Deflection Stress .....	19
	E. Thermal Stress .....	19
	F. Comparison of CW Designs .....	20
VI.	COMPONENTS .....	22
	A. Waterload .....	22
	B. Mode Filters .....	22
	C. Miter Bend .....	22
	D. Flange Adapters .....	23
VII.	TUBE ASSEMBLY .....	24
	A. X-1 (VGE-8060X1) .....	24
	B. X-2 (VGE-8060S1) .....	24
	C. X-3 (VGE-8060S2) .....	24
VIII.	PRELIMINARY TEST RESULTS FOR THE VGE-8060 XN X-1....	25
	A. Hipotting .....	25
	B. Excessive Body Current .....	25
	C. Observation of RF Output .....	25
	D. Control of Operating Parameters .....	26
	E. Preliminary Data .....	27
XI.	PROGRAM SCHEDULE AND PLANS .....	34
X.	REFERENCES .....	41

## LIST OF ILLUSTRATIONS

<u>Figure</u>		<u>Page</u>
1.	Upper Seal Arc .....	4
2.	Lower Seal Arc .....	5
3.	Cathode Arc to Ground .....	7
4.	Parameter Space - VGA-8000 S/N 11 CW .....	8
5.	Parameter Space - VGA-8000 S/N 9 - Pulsed 2.4% Duty .	10
6.	Power and Frequency Sensitivity to Main Magnet No. 3 Current .....	11
7.	Computed VSWR vs Frequency for Beryllia Double Disc Window Designs .....	16
8.	Computed VSWR vs Frequency for Alumina Double Disc Window Designs .....	17
9.	Operating Frequency vs Top Coil Current for X-1 ....	28
10.	Peak Output Power vs Top Coil Current for X-1 .....	29
11.	Peak Output Power vs Bucking Coil Current for X-1 ...	30
12.	Peak Output Power vs Beam Current for X-1 .....	32
13.	Milestone Chart and Status Report .....	35

## I. INTRODUCTION

The objective of this program is to develop a microwave oscillator designed to produce 200 kW of CW output power at 60 GHz. Neither tunability nor bandwidth are considered important parameters in the design but efficiency is. Mode purity in the output waveguide is not a requirement for the device, but the circular electric mode is considered desirable because of its low loss properties.

With these objectives in mind, an approach based on cyclotron resonance interaction between an electron beam and microwave fields is being pursued. The detailed arguments leading to this approach are contained in the final report of a preceding study program<sup>1</sup>. The device configurations of particular interest, called gyrotrons, have been discussed in recent literature<sup>2-6</sup>. They employ a hollow electron beam interacting with cylindrical resonators of the TE<sub>0M1</sub> class.

The optimum beam for the cyclotron resonance interaction is one in which the electrons have most of their energy in velocities perpendicular to the axial magnetic field. Another requirement is that the spread in the axial components of the electron velocities be as small as possible.

The approach chosen to generate the beam is a magnetron type of gun as is used on the 28 GHz gyrotron, also developed for Oak Ridge National laboratory<sup>7,8</sup>. With this type of gun, the shaping of the magnetic field in the gun region becomes quite important.

Gyrotron behavior studies utilizing 28 GHz test vehicles are continuing. Areas studied this quarter included high voltage gun arcing, new cathode materials, rf behavior and cavity and output taper design.

The superconducting solenoid magnet was corrected and operated in support of experimental tube testing.

Preparation was made for making computer calculations of heat transfer and temperature cycle data for the gyrotron collector with pulse lengths relevant for fusion experiments.

Several face cooled double disc CW window designs were evaluated theoretically.

A variety of waveguide components including waterloads, mode filters, miter bends and flange adapters were designed and are in various stages of fabrication.

The first experimental tube yielded promising results in terms of demonstrating the peak output power. The second experimental tube is nearing completion. The third experimental tube is under construction.

## II. GYROTRON BEHAVIOR STUDY

### A. ARCING AND CROWBAR INVESTIGATION

A majority of the quarter was spent working with various tubes and trying to find a cause for the frequent crowbars in the VGA-8000 and VGA-8050 tubes. The purpose of this work is to eliminate some of the design problems in gyrotrons so the developmental work at higher frequencies can proceed more rapidly. Work was completed on the first stage of this investigation.

During this quarter four antennas were placed in the oil tank near the gyrotron gun to look for rf in the gun region. At first it seemed that the rf preceded the tube fault. Further investigation, using a digital storage scope with 50 nanoseconds per point speed, showed that the rf actually followed the gun anode arc by 100-200 nanoseconds. This rf could be due to the high beam current drawn when the gun anode voltage approaches ground potential.

Using the table of probable events that would occur with various tube faults, all types of faults were seen. Observed were the following:

1. gun anode arc to ground (Figure 1);
2. gun anode arc to cathode (Figure 2);
3. cathode arcs to ground with the gun anode following (Figure 3);

These three figures were taken with the digital storage scope during the CW operation of the VGA-8000 S/N 11. Figure 1 shows the mod-anode voltage going quickly towards ground potential while at the same instant the mod-anode current goes in the direction of discharging the capacitance in the modulator between mod-anode and anode. As can be seen in Figure 1 the time constant for the discharging of that capacitance is quite long. Figure 2 shows a lower seal arc. This seems to be much less frequent than an upper seal arc. In this figure the mod-anode voltage tries to go more negative

ORNL Dwg. 81-16816 FED

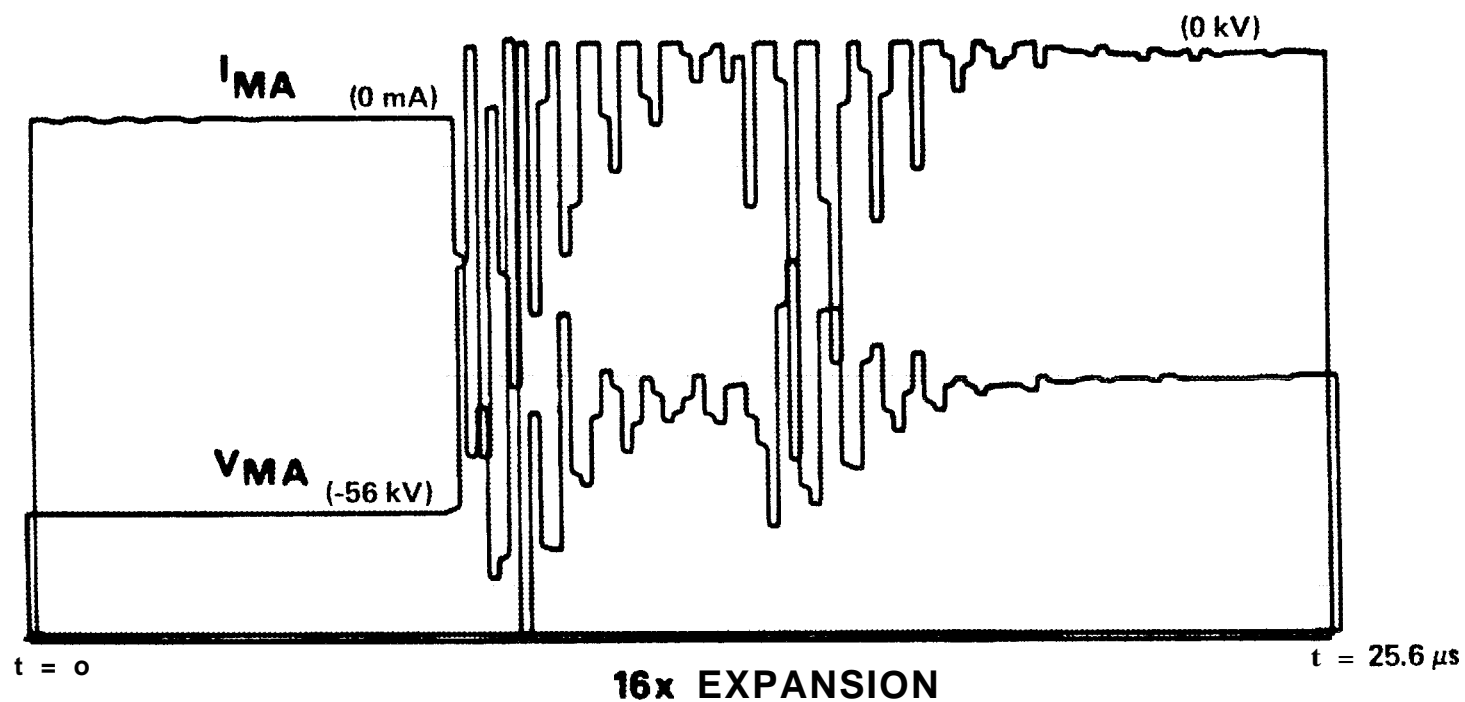


FIGURE 1. UPPER SEAL ARC

ORNL Dwg. 81-16817 FED

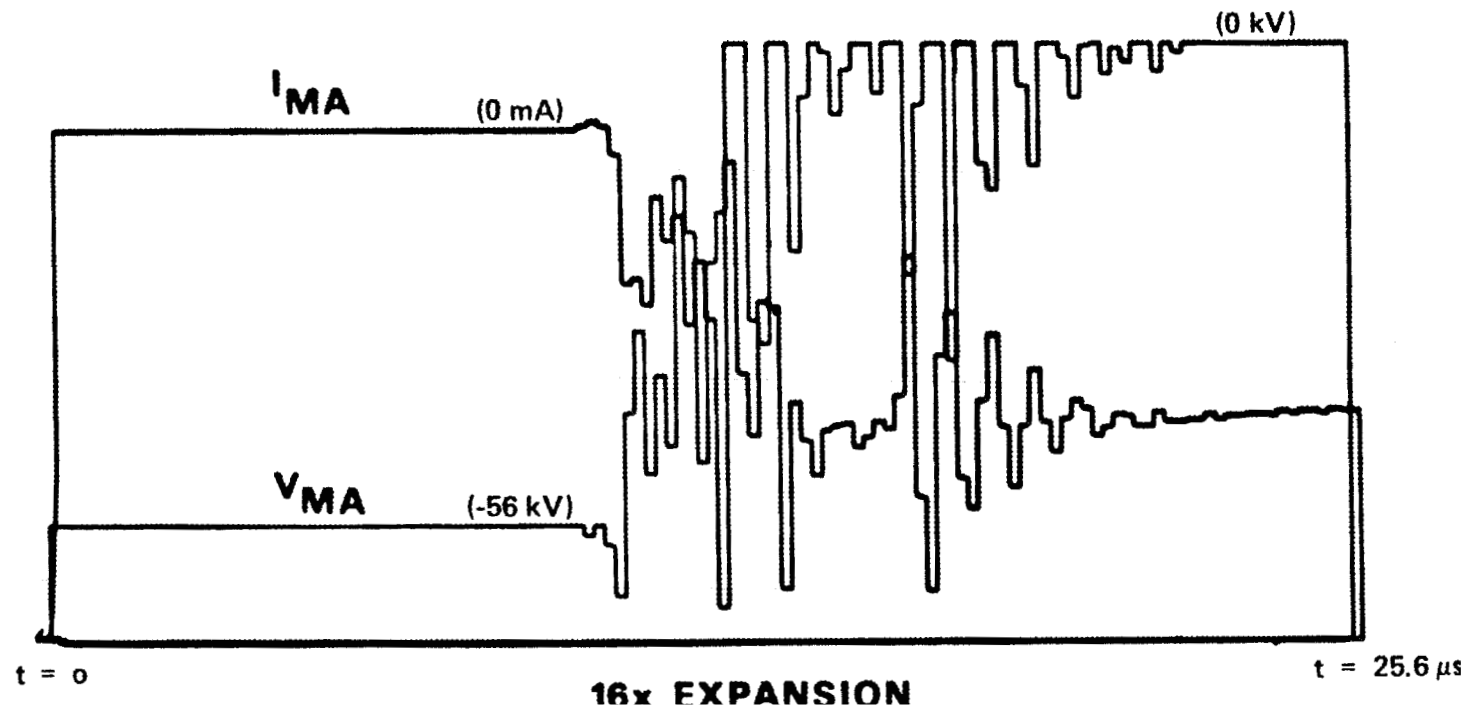


FIGURE 2. LOWER SEAL ARC

and at the same instant the current goes for a short time in the direction of charging the capacitance in the modulator from mod-anode to anode. The crowbar then fires and the voltages go to zero. Figure 3 shows an arc from cathode to ground. This is very seldom seen. The mod-anode voltage goes towards the cathode voltage, and yet the mod-anode current is going in the direction of discharging the mod-anode to anode capacity in the modulator.

In the event of case No. 2, the beam should shut off without a crowbar, but this doesn't seem to be the case, and this will be further investigated. During pulse operation, the gun anode voltage tends to go more negative, rather than more positive, with the start of the crowbar. While in CW operation the failure mode seems to be the gun anode voltage going more positive, indicating an arc from gun anode to ground.

#### B. NEW CATHODE MATERIAL

Discussions were held with those involved in cathode design at Varian. Some data were obtained on results from the cathode study programs at Varian and elsewhere. The M-type and mixed-metal-matrix cathodes appear to be worthy of investigation. They can have lower work functions than the barium cathodes as well as higher emission density with good life. The M-type cathodes typically seem to have a more uniform surface emission, which is good for lower velocity spreads due to surface roughness and spotty emission.

A more thorough study could be made by building an Auger microscope and observing the uniformity of emission. This could be done on a modest budget; but the real question arises in the velocity spread. This measurement would require building a good beam analyzer. At the moment, none exists for magnetron injection guns and construction of a beam analyzer would require a substantially large budget.

#### C. RF BEHAVIOR

During the quarter an exploration of parameter space was performed with two tubes. The data for the CW tube are shown in Figure 4. The VGA-8000

ORNL Dwg. 81-16818 FED

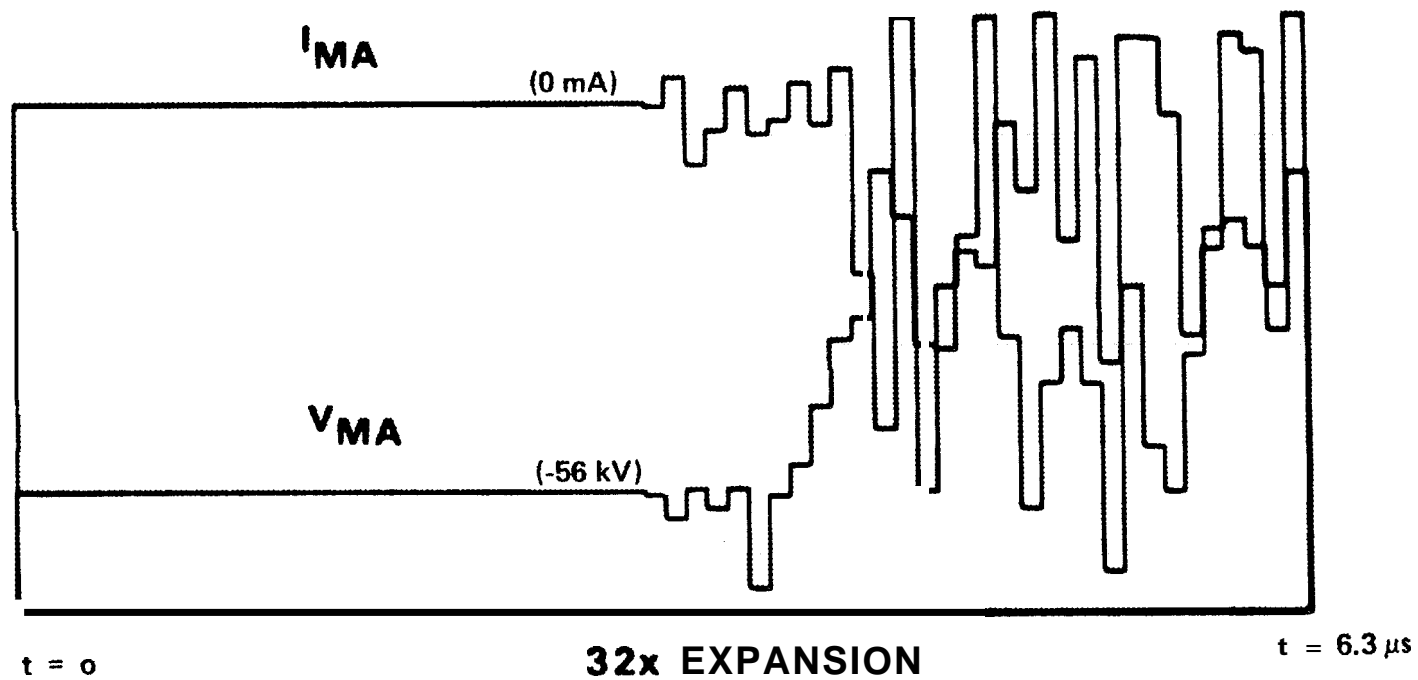


FIGURE 3. CATHODE ARC TO GROUND

ORNL Dwg. 81-16819 FED

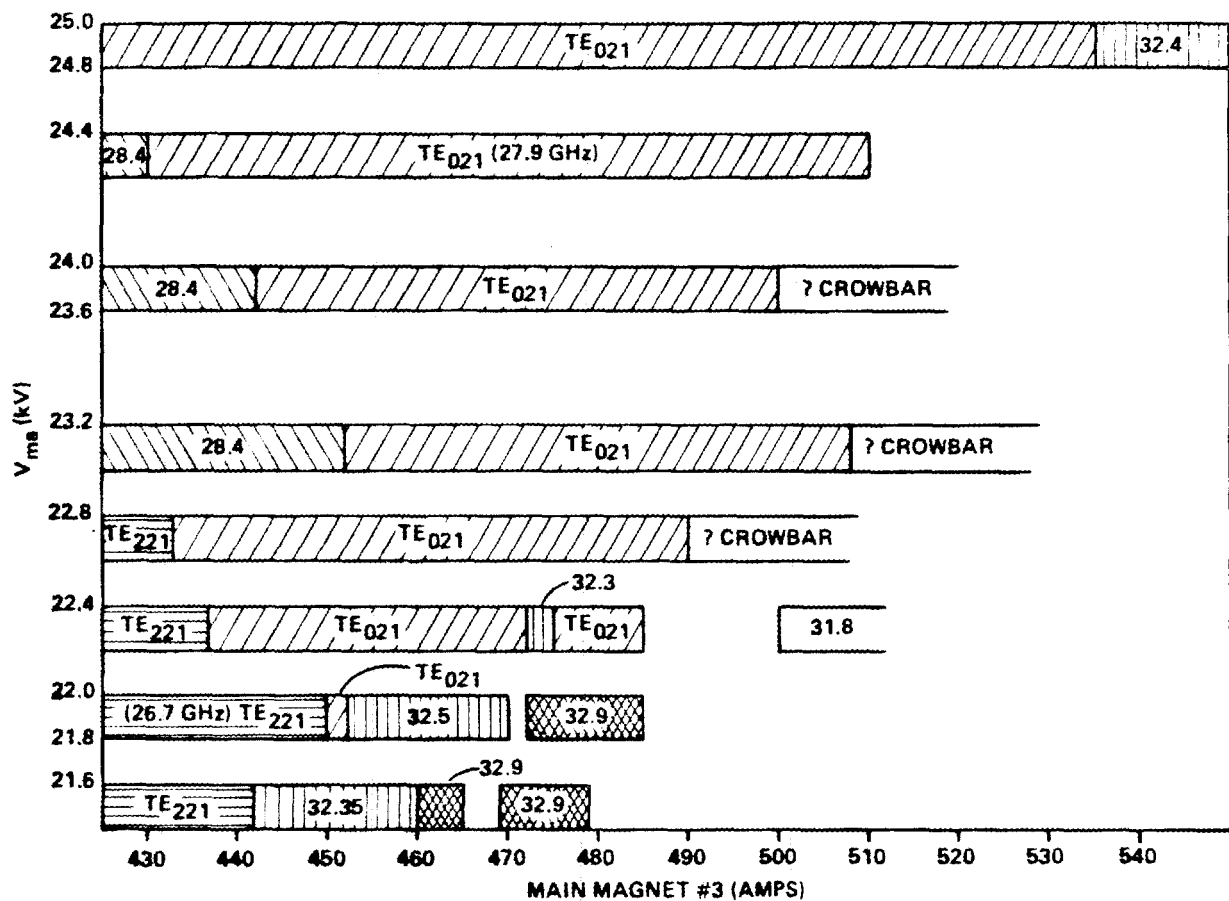


FIGURE 4. PARAMETER SPACE – VGA-8000 S/N 11 CW

S/N 11 was used for these tests. Figure 4 points out that the best way to start the tube oscillating in the correct mode is to start with a low gun anode voltage and a high magnetic field, then raise the gun anode voltage to the design value and then lower the magnetic field to get the desired output power. Figure 5 shows the data for the VGA-8050 S/N 9 pulse tube.

Comparing Figures 4 and 5 illustrates that the operation of the CW and pulse tubes is very similar, but there are two evident differences. First, the CW tube has a 28.4 GHz mode and the pulse tube does not. Further examination will have to be done to identify this mode. Though it is not shown in Figure 4, the  $TE_{221}$  mode was at lower magnetic field than the 28.4 GHz and  $TE_{021}$  modes, as it is also at lower field than the  $TE_{021}$  mode in the pulse tube. The second difference occurs at the low gun anode voltage levels. In the CW case, it appears more difficult to operate in the correct mode than in the pulse case. A plot similar to these with the VGA-8000 S/N 11 operated in the pulse mode will help indicate whether these differences are due to the geometry differences or to the different mode of operation.

At high magnetic fields the 32.4 GHz mode oscillates with low power. This mode does not seem to be a problem because it can be avoided with the appropriate magnetic field setting. The  $TE_{221}$  mode appears to be a more serious problem. As can be seen in Figure 6, to obtain high output power the main field is lowered and then the  $TE_{221}$  mode becomes the lower limit in main magnet field, and the upper limit for power output.

Figure 6 shows the characteristics of the VGA-8000 S/N 11. It was operated for periods of a few hours at the 200 kW CW level. This curve compares well with the previous curves for S/N 5R2 and S/N 6. This tube achieved 40% efficiency.

#### D. CAVITY AND OUTPUT TAPER DESIGN

Two cavity designs have been looked at to reduce the mode competition. One design has already been used on 60 GHz and has been reported. Another design is still being investigated to be used on the VGA-8000 S/N 8 rebuild.

ORNL Dwg. 81-16820 FED

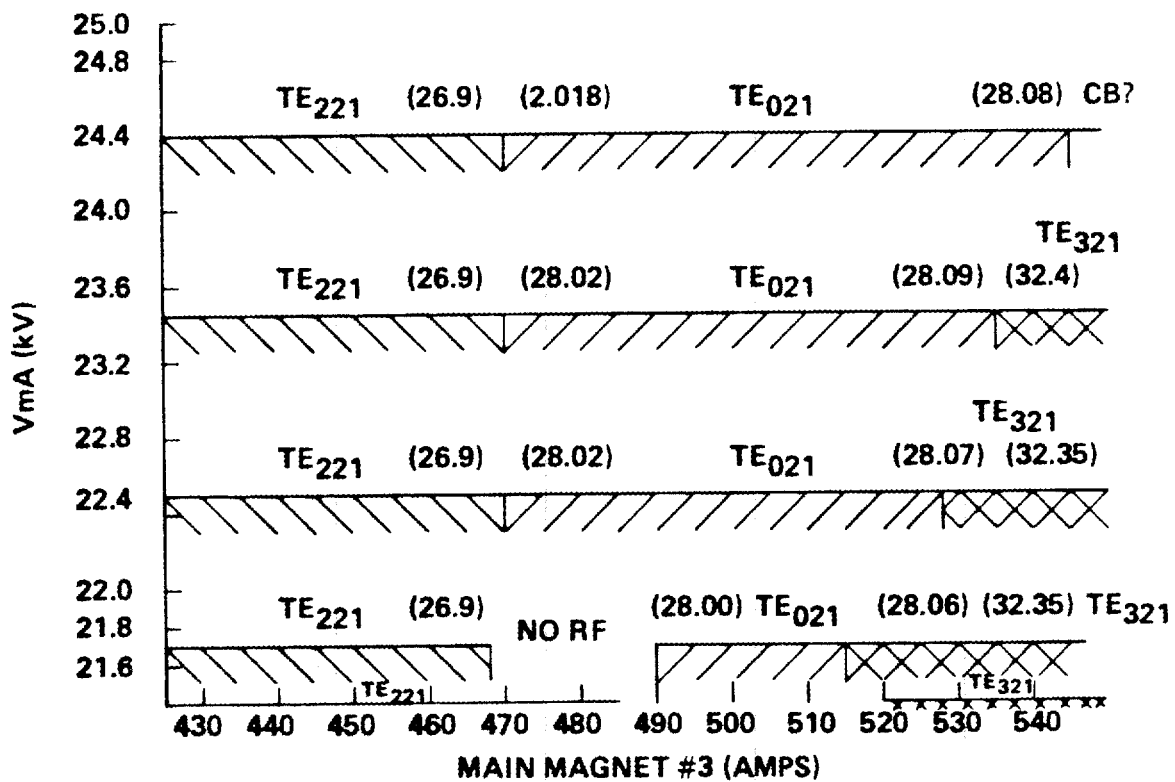


FIGURE 5. PARAMETER SPACE – VGA-8000 S/N 9 – PULSED 2.4% DUTY

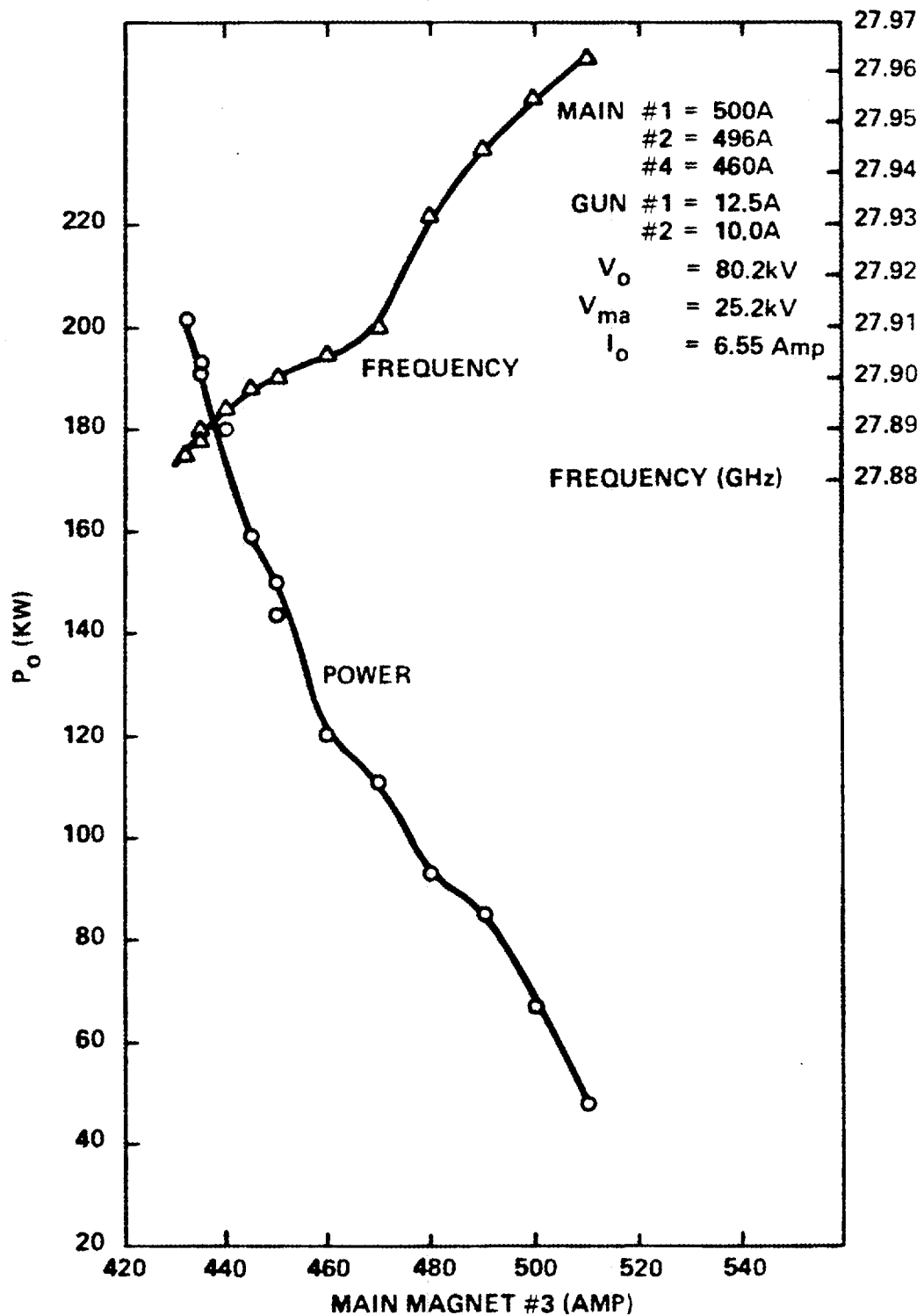
VGA-8000 S/N 11 – CW  
POWER VS MAIN MAGNET #3

FIGURE 6. POWER AND FREQUENCY SENSITIVITY TO MAIN MAGNET NO. 3 CURRENT

The rebuild of S/N 8 will also include a part for a residual gas analyzer (RGA). This will allow the liberated gases to be analyzed during bakeout as well as during tube operation. There will also be another port to observe the gas pressure in the gun region during operation. These diagnostics will help to determine what is occurring in the tube during operation.

### III. SUPERCONDUCTING SOLENOID MAGNET

The superconducting solenoid magnet, received at the end of December, exhibited some dimensional problems. The short cylindrical section of the bore which mates with the O-ring at the bottom of the tube body and provides alignment was undersized, tapered and out of round. This condition likely occurred during welding of the plate and shell dewar assembly. An in-process machine operation was apparently omitted.

This mechanical problem, which prevented inserting the gyrotron completely through the bore of the dewar, was solved at Varian by setting up the entire dewar in a mill and boring out the inside surface to the correct diameter.

After evacuating the vacuum chamber of the dewar, the boil-off of liquid helium and liquid nitrogen was approximately as expected.

An axial magnetic field measurement was made at Varian that agreed with the field measurement at the vendor and with calculations.

The only remarkable electrical problems involved the time required to change the magnetic field. The coils were designed to operate a 110 GHz gyrotron. Consequently they have more inductance than absolutely necessary to operate a 60 GHz gyrotron. This problem will be alleviated by introducing a suitable resistance in series with the power supplies and main coils.

During initial tube operation it was found necessary to trim the mechanical axis of the gyrotron with respect to the mechanical axis of the dewar to improve beam transmission.

It is understood that this discrepancy is associated with the mechanical support consistent with high performance boil-off characteristics.

#### IV. COLLECTOR

Preliminary heat transfer calculations presented in the last quarterly report<sup>9</sup> suggest that more detailed, computer calculations be performed to determine behavior at the water channel. The temperature as a function of position and time, both during and after a pulse, will be required for stress calculations to determine the suitability of the collector for repeated long pulse operation and also for determining required collector cooling water flow rates for less than continuous operation.

Proposals were solicited for performing these calculations from outside vendors, one of whom had been used for performing CW burnout calculations during the 28 GHz gyrotron development. Approximately half the cost of the proposed effort was for computer time. A decision was made to utilize the Magnetic Fusion Energy computer network. A code entitled TACO is being used to perform the thermal analysis.

## V. CW WINDOW DESIGNS

During the quarter, further effort was applied to the CW window design problem for the 60 GHz 200 kW CW oscillator. Investigation of the electrical properties (bandwidth and dielectric loss) as well as the mechanical properties (deflection and thermal stress) of double disc FC-75 face-cooled window assemblies was carried out. A summary of the design results is given in Table 1 for six different assemblies employing both beryllia and alumina discs.

### A. LOCATION OF PASSBANDS

For each of the six designs presented in Table 1, the gap size was optimized to provide a perfect match at the operating frequency of the VGE-8060 S/N X-1, namely 59.7 GHz. The experimental tube also tended to jump into an undesired mode, probably the  $TE_{221}$ , at a frequency of 57.7 GHz. For this reason it is desirable to match the CW window assembly for this frequency as well as the desired frequency. The computed VSWR is plotted versus frequency in Figures 7 and 8 for each of the window designs under consideration. Characteristically, the CW window passband takes a double notch form as shown in Figures 7 and 8. It is possible, by choosing an appropriate window thickness, to approximately center one passband on each of the frequencies observed with X-1. The double disc window with  $5/2 \lambda$  alumina discs is one such configuration as described in Table 1.

### B. BANDWIDTH

The bandwidth of each passband should be as wide as possible, but in any case, must exceed the oscillator resonance bandwidth,  $f/Q$ . This criterion implies an upper limit on the allowable electrical thickness of the CW window assembly. All the designs listed in the table meet this bandwidth criterion. However, the  $5/2 \lambda$  alumina window assembly appears to have reached the absolute limit in electrical thickness as it provides a passband for a VSWR of 1.2:1 of only 300 MHz.

ORNL Dwg. 81-16822 FED

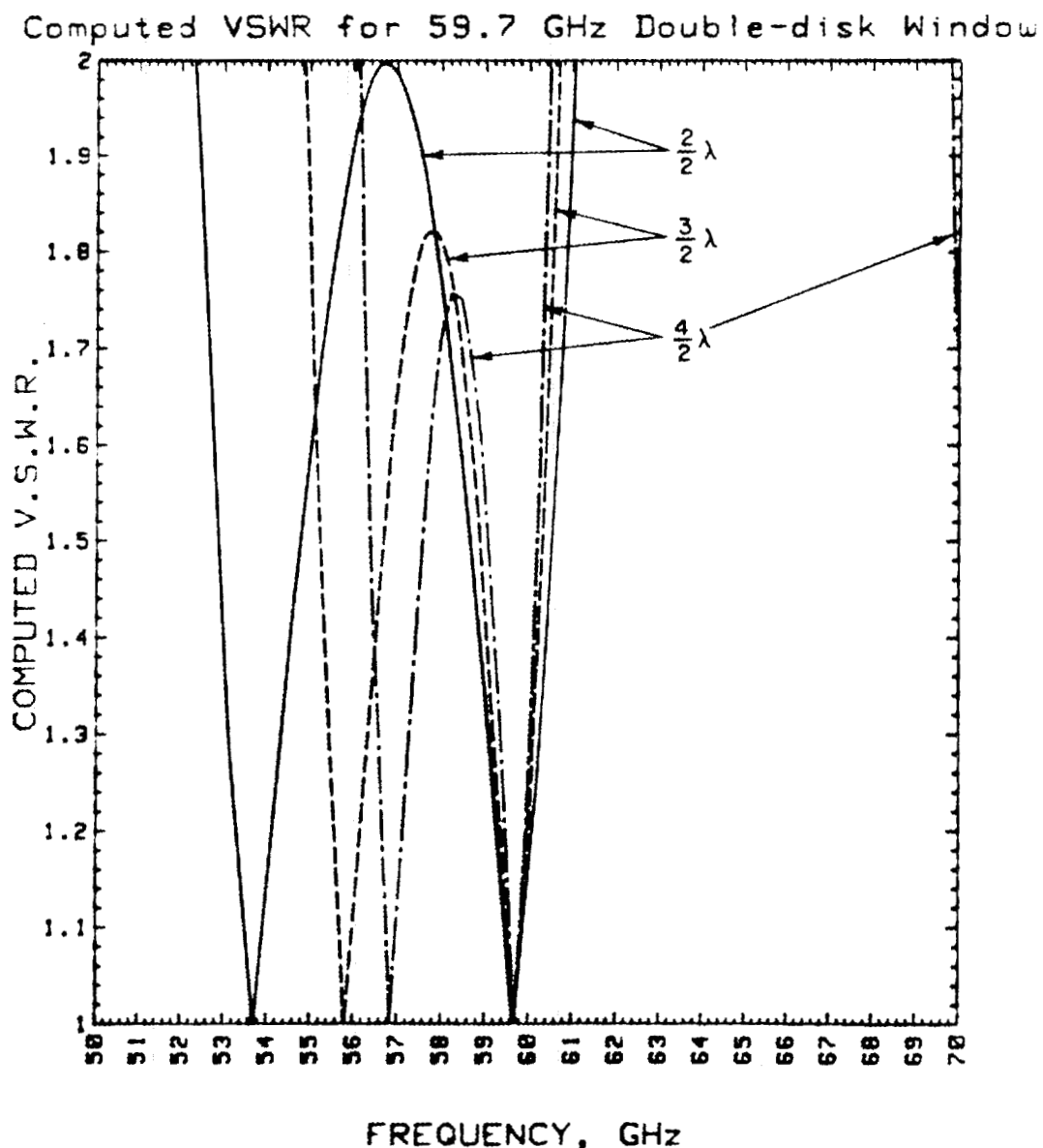


FIGURE 7. COMPUTED VSWR vs FREQUENCY FOR BERYLLIA DOUBLE DISC WINDOW DESIGNS

ORNL Dwg. 81-16823 FED

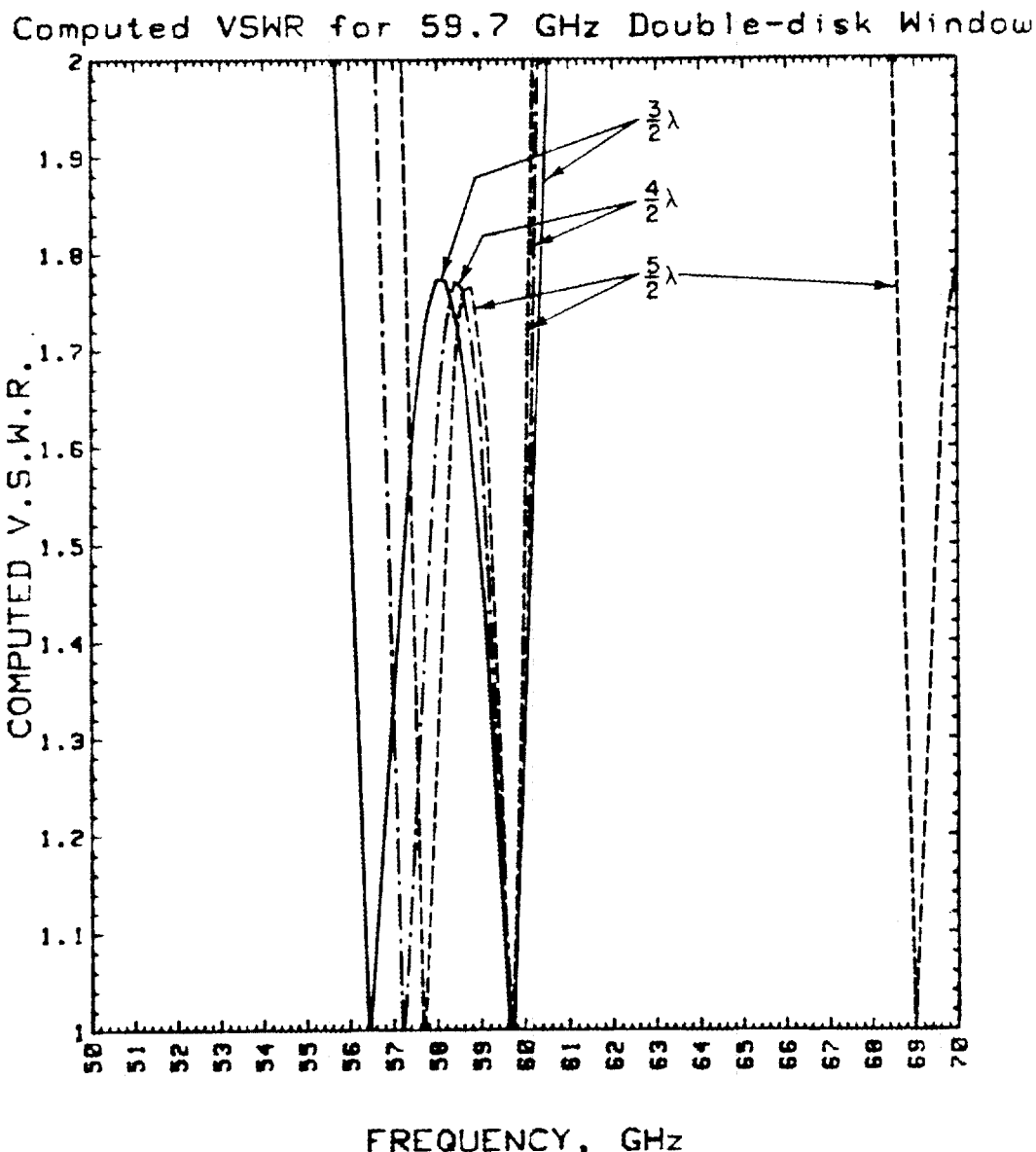


FIGURE 8. COMPUTED VSWR vs FREQUENCY FOR ALUMINA DOUBLE DISC WINDOW DESIGNS

Table 1  
60 GHz Double Disc Window Designs

Double Disc Configuration				Electrical Properties			Mechanical Properties			
Disc Material	Disc Thickness (inches)		PC-75 Gap (inches)	TE <sub>021</sub> Bandwidth for VSWR = 1.2 (MHz)		Window Assy VSWR	Loss (kW)	Deflection @ 30 psig (inches)	Deflection Stress (psi)	Thermal Stress (psi)
Beryllia	2/2 $\lambda$	0.083	0.028	760	1.85	2.1	0.0026	12,800	92	
Beryllia	3/2 $\lambda$	0.120	0.033	570	1.82	2.6	0.0008	6,100	190	
Beryllia	4/2 $\lambda$	0.157	0.039	470	1.59	3.1	0.0004	3,600	330	
Alumina	3/2 $\lambda$	0.099	0.036	500	1.71	2.3	0.0017	9,000	740	
Alumina	4/2 $\lambda$	0.131	0.036	420	1.40	2.4	0.0007	5,100	1,300	
Alumina	5/2 $\lambda$	0.163	0.036	300	1.10	2.5	0.0004	3,300	2,000	

### C. DIELECTRIC LOSS

The power lost in these window assemblies through dielectric dissipation is expected to be higher than that observed at 28 GHz because the window thicknesses, in numbers of half wavelengths, are larger. All the window assemblies considered in Table 1 should exhibit dissipation in the range of 2-3 kW, most of which is due to dielectric loss in the FC-75 coolant itself. As the amount of loss is similar for all the designs considered, this property does not present any strong argument in favor of any particular design. It is noted, however, that because beryllia has a higher loss tangent than alumina, the dissipation in the beryllia assemblies will be slightly higher than in the alumina assemblies.

### D. DEFLECTION STRESS

There are two major sources of stress on the ceramic discs in these CW window designs. There is a deflection, and therefore a restoring deflection stress, caused by the load of the pressurized FC-75 distributed across the face of each disc. The disc on the vacuum side must, in addition, withstand the load of atmospheric pressure. When running with an FC-75 pressure of 30 psig the load on the vacuum side disc will be 45 psi absolute load pressure. This leads to a deflection and deflection stress at the center of the window as listed in Table 1. Excessive deflections are encountered when the discs are less than one tenth of an inch in thickness.

### E. THERMAL STRESS

As the heat dissipated in the ceramic diffuses toward the coolant, the temperature difference between the disc faces induces a thermal stress in the ceramic. Beryllia, because of its excellent thermal conductivity, is subject to an order of magnitude less thermal stress than alumina. For a given ceramic material the temperature difference between the disc faces are higher for thicker discs, although the thermal stress remains within safe limits for all of the designs in Table 1. When both thermal and deflection stress are considered together there is a narrow range of disc thicknesses which simultaneously permit low deflection and low thermal stresses.

F. COMPARISON OF CW DESIGNS

The window designs of Table 1 have been rated against the criteria described above as shown in Table 2. The labels, "unacceptable", "marginal", and "acceptable" are applied to those window properties which differ significantly amongst the designs under consideration. According to the rating system, the  $5/2 \lambda$  alumina window is the clear winner for the first 60 GHz CW window design although it has the disadvantage of a narrow  $TE_{02}$  bandwidth for the passband centered at 59.7 GHz. Once the window assembly is completed it may be necessary to retune the window slightly by adjusting the FC-75 gap size in order to provide a perfect match for the  $TE_{02}$  mode at 59.7 GHz.

Table 2  
Design Trade-offs for 60 GHz CW Window Design

Property	Beryllia			Alumina		
	2/2 $\lambda$	3/2 $\lambda$	4/2 $\lambda$	3/2 $\lambda$	4/2 $\lambda$	5/2 $\lambda$
TE <sub>021</sub> , bandwidth	Acceptable	Acceptable	Marginal	Marginal	Marginal	Marginal
TE <sub>221</sub> VSWR	Unacceptable	Unacceptable	Unacceptable	Unacceptable	Marginal	Acceptable
Deflection	Unacceptable	Acceptable	Acceptable	Unacceptable	Acceptable	Acceptable
Deflection Stress	Unacceptable	Marginal	Acceptable	Unacceptable	Marginal	Acceptable

## VI. COMPONENTS

A variety of waveguide components is being developed for use with the 60 GHz gyrotron including a waterload, mode filters, miter bend and flange adapters.

### A. WATERLOAD

A CW waterload has been designed. All parts have been ordered and almost all of them have been received. Construction of the first CW waterload is scheduled to begin in mid April.

### B. MODE FILTERS

Two types of mode filters have been designed. The first is a water-cooled stainless steel waveguide, which utilizes the differential in loss between non-circular electric modes and circular electric modes. All parts for this mode filter have been ordered and received. Assembly of the first mode filter began in late March.

The second type of mode filter consists of alternating stainless steel rings and gaps backed up by a waterloaded ceramic cylinder. In addition to the differential filtering loss mechanism of the first type of filter, the second type creates breaks in the conducting wall for non-circular electric modes but not for circular electric modes. All parts for this mode filter have been ordered and almost all of them have been received. Construction of this type of mode filter is expected to begin in mid April.

### C. MITER BEND

A mitered 90° circular waveguide bend has been designed for potential waveguide configuration tests. All parts have been ordered and received. Assembly of the first miter bend began in late March.

D. FLANGE ADAPTERS

Adapters have been designed to enable connection from the copper gasketed flange to either of the male and female designs used at 28 GHz. This will allow use of certain waveguide component designs developed on the 28 GHz program. All parts for both the male and female flange adapters have been ordered and received. Construction began in late March.

## VII. TUBE ASSEMBLY

### A. X-1 (VGE-8060X1)

The first 60 GHz experimental gyrotron was pinched off on January 8 and placed in test on February 6. This tube utilizes an uncooled anode, a small collector and a single disc beryllia window. The main purpose of the tube is to demonstrate 200 kw of peak output power at 60 GHz. Early test results are described in Section VIII.

### B. X-2 (VGE-8060S1)

The second experimental tube incorporates a water-cooled anode and a dimensional change to place the cathode in a more favorable location with respect to the magnetic field. All major assemblies are complete. Final assembly will start immediately. The tube will be available for test after test set modification. The purpose of this tube is to demonstrate 200 kw of peak power at fusion experiment relevant pulse durations of at least 100 ms.

### C. X-3 (VGE-8060S2)

The third experimental tube provides a vehicle for rapidly incorporating design changes suggested by tests of X-1 and X-2. All major assemblies except one collector seal assembly and the anode and cavity assembly are complete. Final assembly will be complete in July.

## VIII. PRELIMINARY TEST RESULTS FOR THE VGE-8060 SN X-1

### A. HIPOTTING

Testing of the first experimental tube was begun during the first week of February. The tube was successfully hipotted to 30 kV across the cathode - gun anode seal and to 100 kV across the gun anode - anode seal. During hipotting a few mild gas bursts were observed at which time it was noted that as the pumps recovered from a gas pressure surge, the indicated pump pressure was two orders of magnitude higher in the gun pump than in the collector pump. This behavior was expected because the low pumping conductance of the beam tunnel effectively isolates one end of the tube from the other.

### B. EXCESSIVE BODY CURRENT

Pulsed beam power was applied during the second week of February and by comparing body current and beam current it was determined that beam interception in the beam tunnel was excessive. While the magnet steering coils did have a slight effect in reducing the body current, their ampere-turns rating was insufficient to steer the beam clearly through the beam tunnel. To correct this problem, attempts to shield the tube from external magnetic perturbations by wrapping iron shields around both ends of the magnet dewar were made. This had no effect on the excessive beam interception. Finally, the tube was tilted about a pivot point near the gun by using a mechanical adjustment on the plate which supports the tube at the top of the dewar. A transverse adjustment of the beam tunnel with respect to the axis of the dewar bore of 0.022" east and 0.015" north was necessary to send the beam through the beam tunnel with acceptable ( $\leq 5$  ma) beam interception at full beam current (8 a).

### C. OBSERVATION OF RF OUTPUT

RF output near 60 GHz was first observed on 24 February. It became immediately apparent that the modulator voltage pulse was not sufficiently flat. Work was done on the voltage divider in the modulator to better

compensate the system for running at 8 a, 80 kV. The gun anode voltage pulse was improved enough to observe rf pulses of ~ 20  $\mu$ sec in duration. However, because this tube appeared to be very sensitive to small changes in gun anode voltage, the rf pulse duration was limited by the slope of the gun anode voltage waveform. Thus, it was not possible to increase the rf pulse duration without further improvement in the flatness of the voltage pulse.

During this portion of the testing, measurements, indicating a peak output power of ~ 200 kW at ~ 50% efficiency were obtained. Some uncertainty must be attributed to these preliminary data because, while average rf power (~ kW) was measured calorimetrically, the inferred peak power depended on the less certain measurement of rf pulse duration. When running under the modulator pulse shape conditions mentioned above, the rf pulse duration was less than the beam pulse duration. This situation might cause significant error in the peak power measurement if, for example, any unobserved rf was put out by the tube at other times during the beam pulse.

#### D. CONTROL OF OPERATING PARAMETERS

In order to improve the accuracy of the rf power measurements it was clear that further improvement in the pulse shape was needed. Additional adjustments on the test set improved the flatness of the gun anode pulse to  $\pm 1\%$ . At this point it became apparent that better control of the voltage pulse amplitude was also necessary in order to be able to tune the tube to the optimum operating point. Drift in the dc beam voltage also worked against tuning the tube to the optimum operating point, indicating that the beam voltage regulation was inadequate. Finally, the bucking coil current and main solenoid coil currents were subject to long settling times (about 10 seconds and 3 minutes, respectively) because of the high load inductance and low series load resistance in the magnet energizing circuits. These system problems will be addressed during the long pulse upgrade of the test set, scheduled for next quarter.

## E. PRELIMINARY DATA

In spite of the complications mentioned above, sufficient preliminary data were obtained during this quarter to identify the basic operating characteristics of this 60 GHz design. The tube was run at 100  $\mu$ sec pulse durations and somewhat lower peak power levels ( $\sim 150$  kW). The data shown in Figures 9 and 10 were obtained with the parameters given in Table 3.

Table 3  
Parameters for Frequency vs Top  
Coil Current

Beam Voltage	$\sim 80$ kV
Beam Current	$\sim 6.1$ A
Gun Anode Voltage	$\sim 18$ kV
Pulse Duration	$\sim 100$ $\mu$ sec
Pulse Repetition Rate	$120$ (sec) $^{-1}$
Bottom Coil	25.51 A
Bucking Coil	2.68 A

Behavior similar to that observed in the 28 GHz experiments was observed here. A decrease in main magnet current detunes the output frequency while it increases the power output. After a sharp peak in output power, the operating frequency jumps to that of another mode, probably the TE<sub>221</sub>, at 57.79 GHz. The parameters given in Table 4 accompany the plot of output power versus bucking coil current shown in Figure 11. As expected, an increase in bucking coil current decreases the magnetic field at the cathode, thereby increasing the transverse energy in the beam and raising the rf output power.

ORNL Dwg. 81-16824 FED

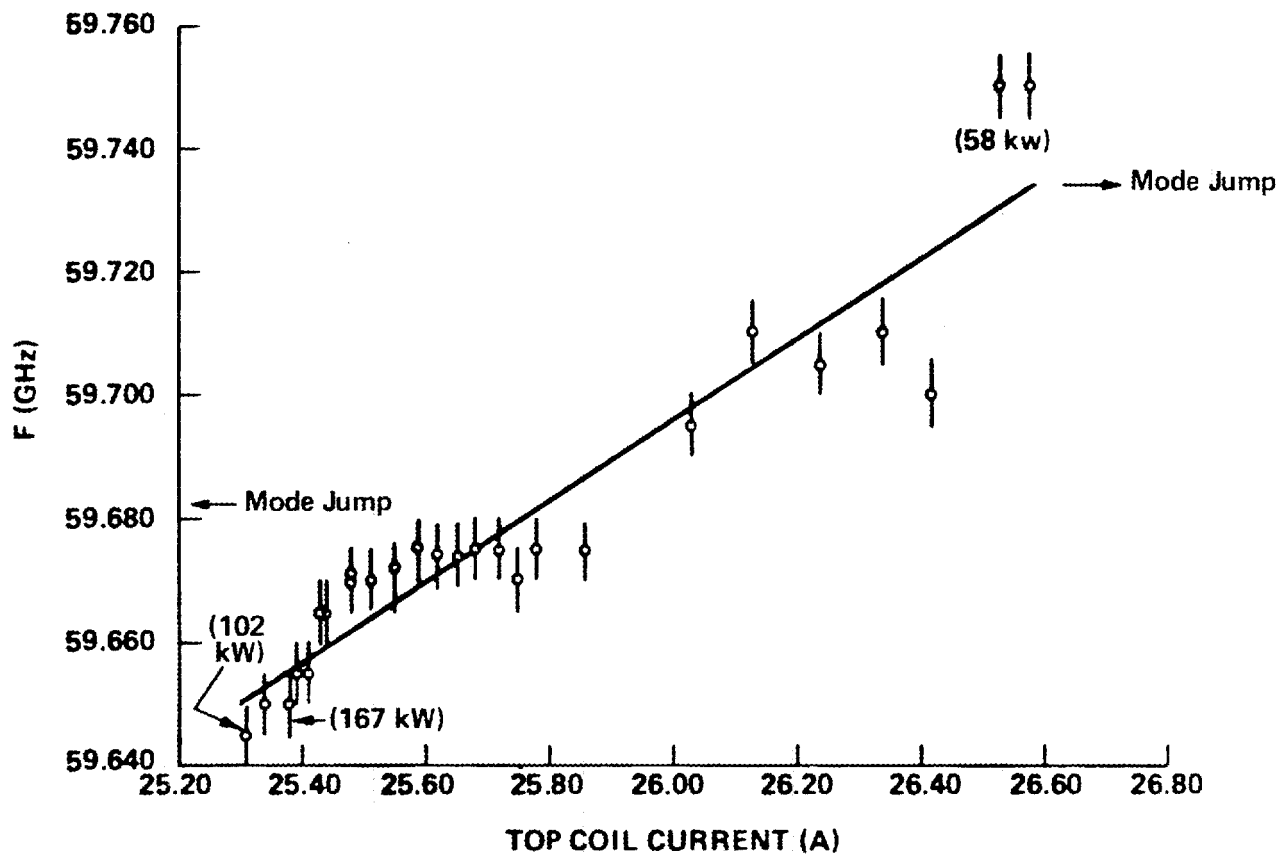


FIGURE 9. OPERATING FREQUENCY vs TOP COIL CURRENT FOR X-1

ORNL Dwg. 81-16825 FED

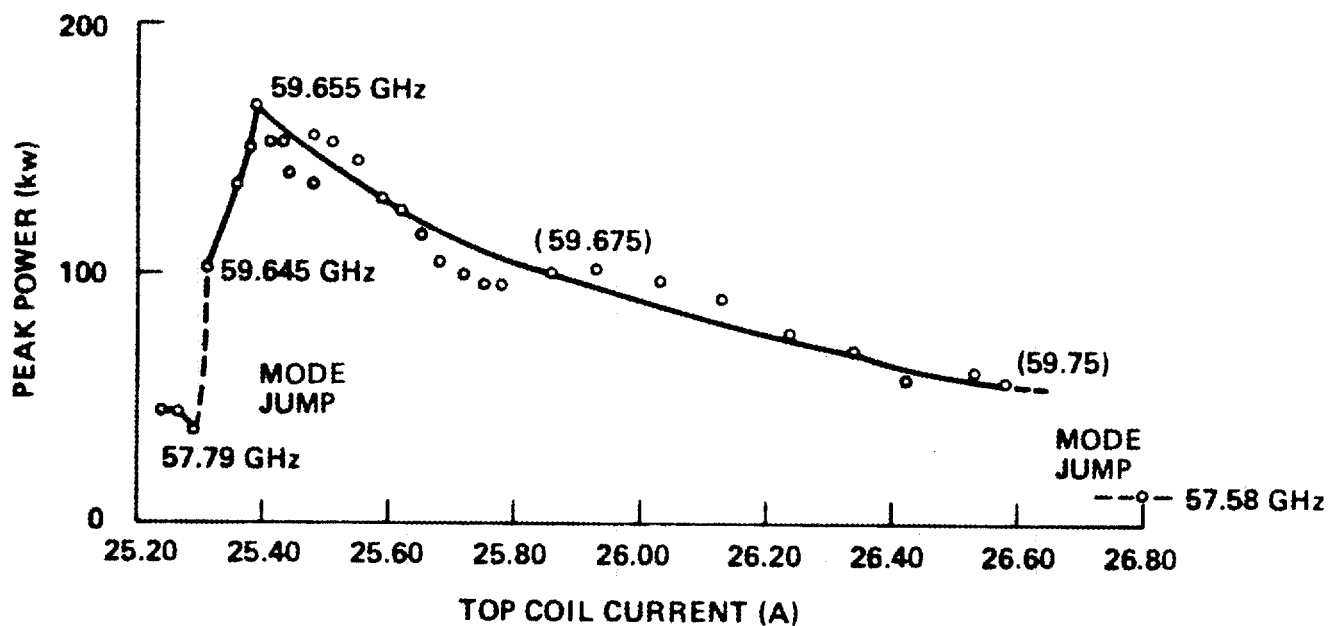


FIGURE 10. PEAK OUTPUT POWER vs TOP COIL CURRENT FOR X-1

ORNL Dwg. 81-16826 FED

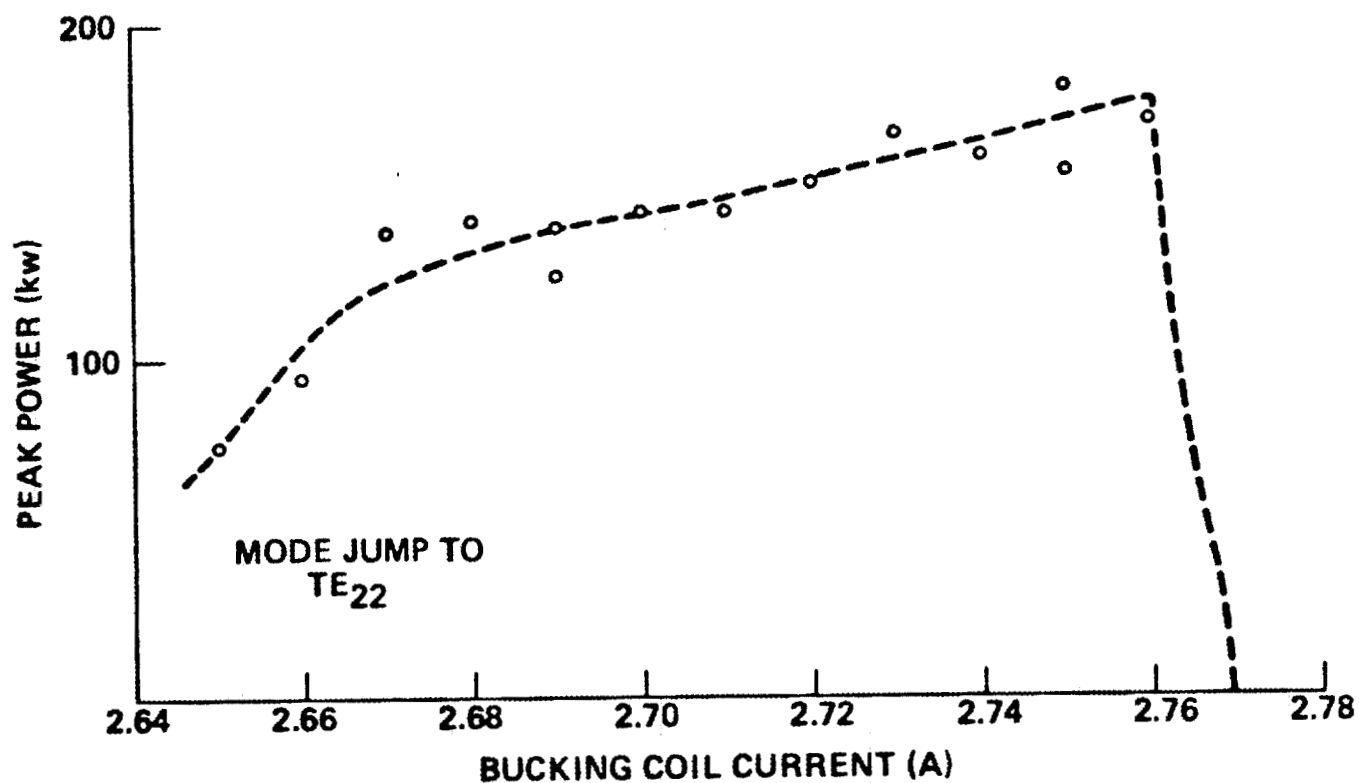


FIGURE 11. PEAK OUTPUT POWER vs BUCKING COIL CURRENT FOR X-1

Table 4  
Parameters for Power vs Bucking  
Coil Current

Beam Voltage	~ 80 kV
Beam Current	~ 6.4 A
Gun Anode Voltage	~ 17.8 kV
Pulse Length	~ 50 $\mu$ sec
Repetition Rate	120 Hz
Top Coil	25.45 A
Bottom Coil	25.51 A

A summary of the data obtained for peak output power versus beam current is shown in Figure 12. These points were obtained over a large range of operating parameters including pulse durations from 20-100  $\mu$ sec. We have compared the data with the performance predicted by Chu<sup>10</sup> for starting current and by Musinovich and Erm<sup>11</sup> for large signal interaction efficiency. The curves were calculated for cavities with Gaussian electric field profiles of  $6\lambda$ ,  $8\lambda$ , and  $10\lambda$  in length using the theoretical results in Reference 11. The experimental data fall roughly in the range of  $6\lambda - 10\lambda$  indicating that our complex tapered cavity is comparable to a Gaussian field profile cavity of length  $\sim 8\lambda$ .

A number of qualitative conclusions may also be drawn from the preliminary test results of this tube:

The sensitivity of the 60 GHz gun performance to variations in gun anode voltage and backing coil current is more pronounced than the 28 GHz guns. This was anticipated because a long cathode gun optics design is being used which is inherently more sensitive to changes in these parameters than the short cathode design employed in the 28 GHz guns.

The mechanical tolerances specified in building the magnet are not sufficient to prevent beam interception in the beam tunnel. When ordering solenoid magnets in the future this problem will be corrected by requiring more ampere-turns for the steering coils, as it is not within the state of

ORNL Dwg. 81-16827 FED

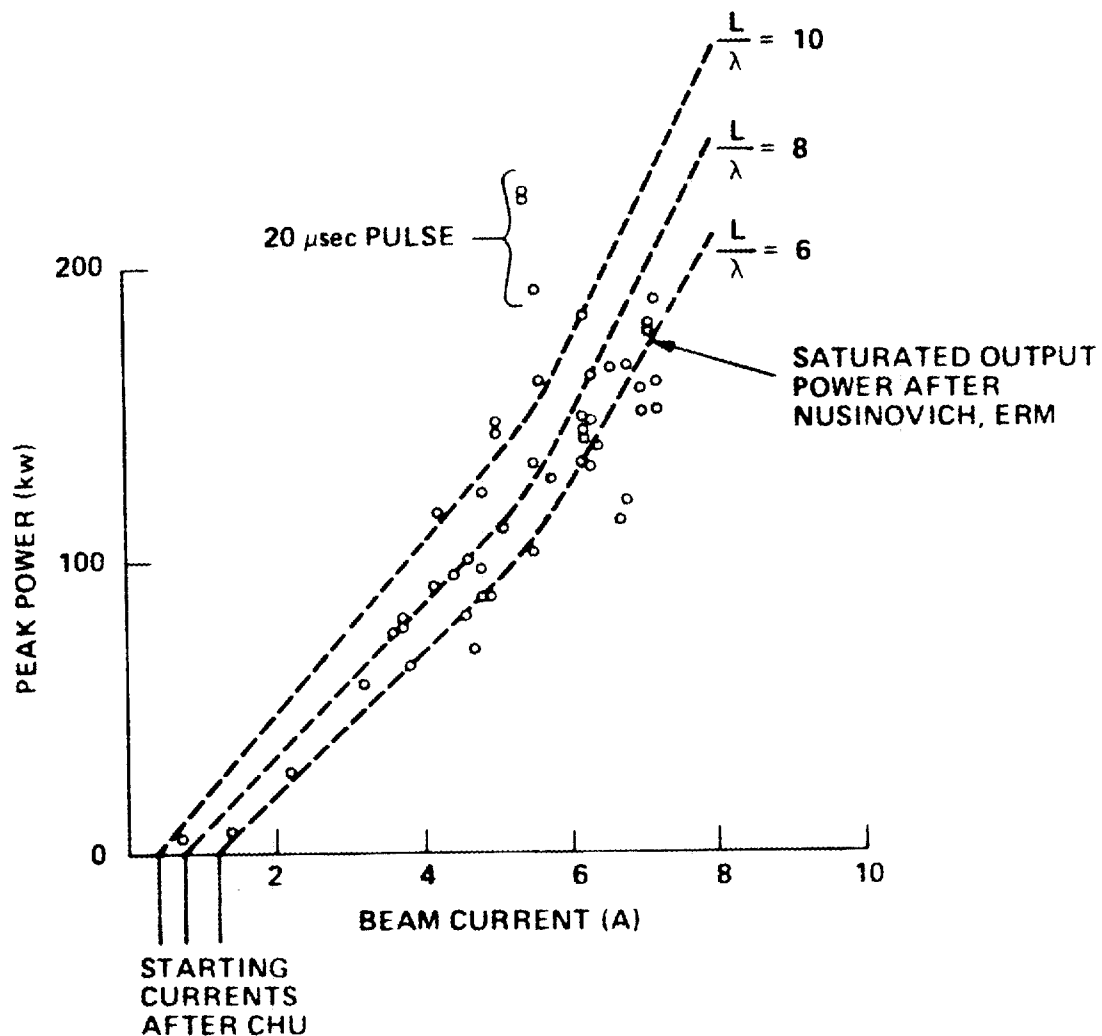


FIGURE 12. PEAK OUTPUT POWER vs BEAM CURRENT FOR X-1

the art to achieve the necessary mechanical tolerances for alignment of the magnetic field with the mechanical axis of the dewar.

The use of a separate vacuum manifold and pump at the gun end of the tube is an important aspect of the 60 GHz tube design. The gun pump provides an interesting diagnostic for the tube during crowbars. Furthermore, although it is too early in the life of the design to draw conclusions about the burn-in behavior of the tube, the gun pump appears to have decreased tube processing time and permitted operation with fewer crowbars than is possible for the 28 GHz tubes.

The values of gun anode voltage and bucking coil current used to achieve optimum rf performance indicate that at present the gun sits too low in the dewar bore. After rechecking all of the design data it was discovered that the tube length between the cavity and the gun was indeed excessive. This error will be corrected on X-2. In any event, it appears that respectable beam quality may be obtained, even when the gun is in the incorrect axial position, by compensating for the error with changes in bucking coil current and gun anode voltage.

## IX. PROGRAM SCHEDULE AND PLANS

The Milestone Chart and Status Report is shown in Figure 13. Preliminary test results on X-1 were encouraging, having demonstrated the peak output power at short pulse durations. About half of the quarter was occupied with test set modification and debugging. X-1 has been used as the test vehicle for this effort. X-2, with a watercooled anode, is nearing completion and will be available for test following test set debugging.

Proposals and quotations for a spare superconducting solenoid magnet have been received and are being evaluated.

The waveguide components required for testing X-1 were completed in time. These consisted of a pulse waterload and a combination frequency sampler and arc detector.

All major assemblies for X-3 except one collector seal and the anode and cavity assembly are complete. Construction of this tube will benefit from lessons learned on X-1 and X-2.

The major subassembly drawings for X-4 are complete. The current plan for this tube is to use a collector large enough in diameter to handle CW operation and an FC-75 face cooled double disc window. The final assembly drawing for this tube will be complete early next quarter. Parts fabrication will also start next quarter.

Construction of deliverable waveguide components will also start next quarter.

The gyrotron behavior investigation will continue next quarter utilizing 28 GHz test vehicles. The arcing and crowbar investigation will be complete next quarter. Among the other investigations to be completed next quarter are ones on new cathode materials, parameter space, rf output stability, low level starting and efficiency. It is expected that one tube modification, processing study and test cycle will be completed in support of this portion of the program.

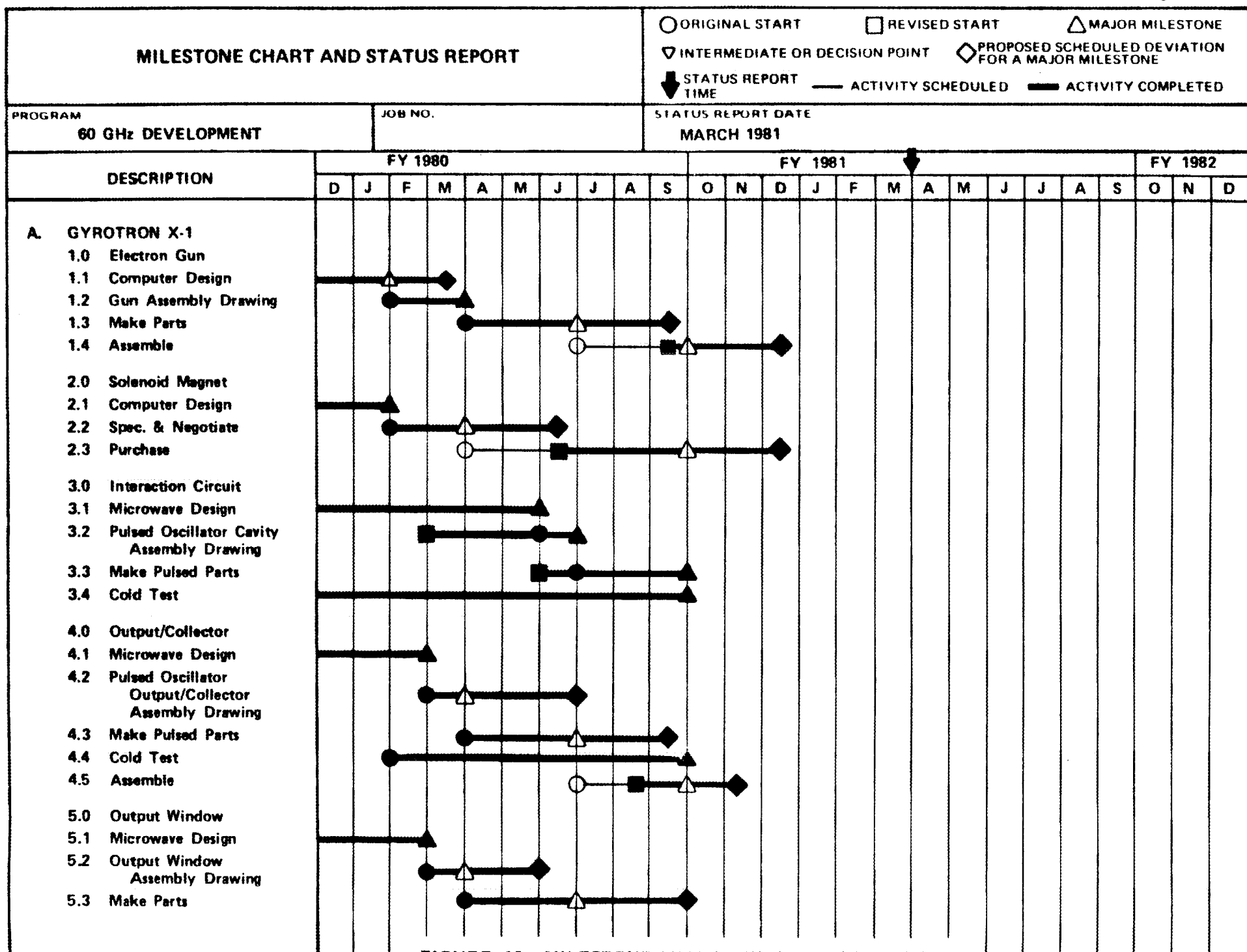


FIGURE 13. MILESTONE CHART AND STATUS REPORT

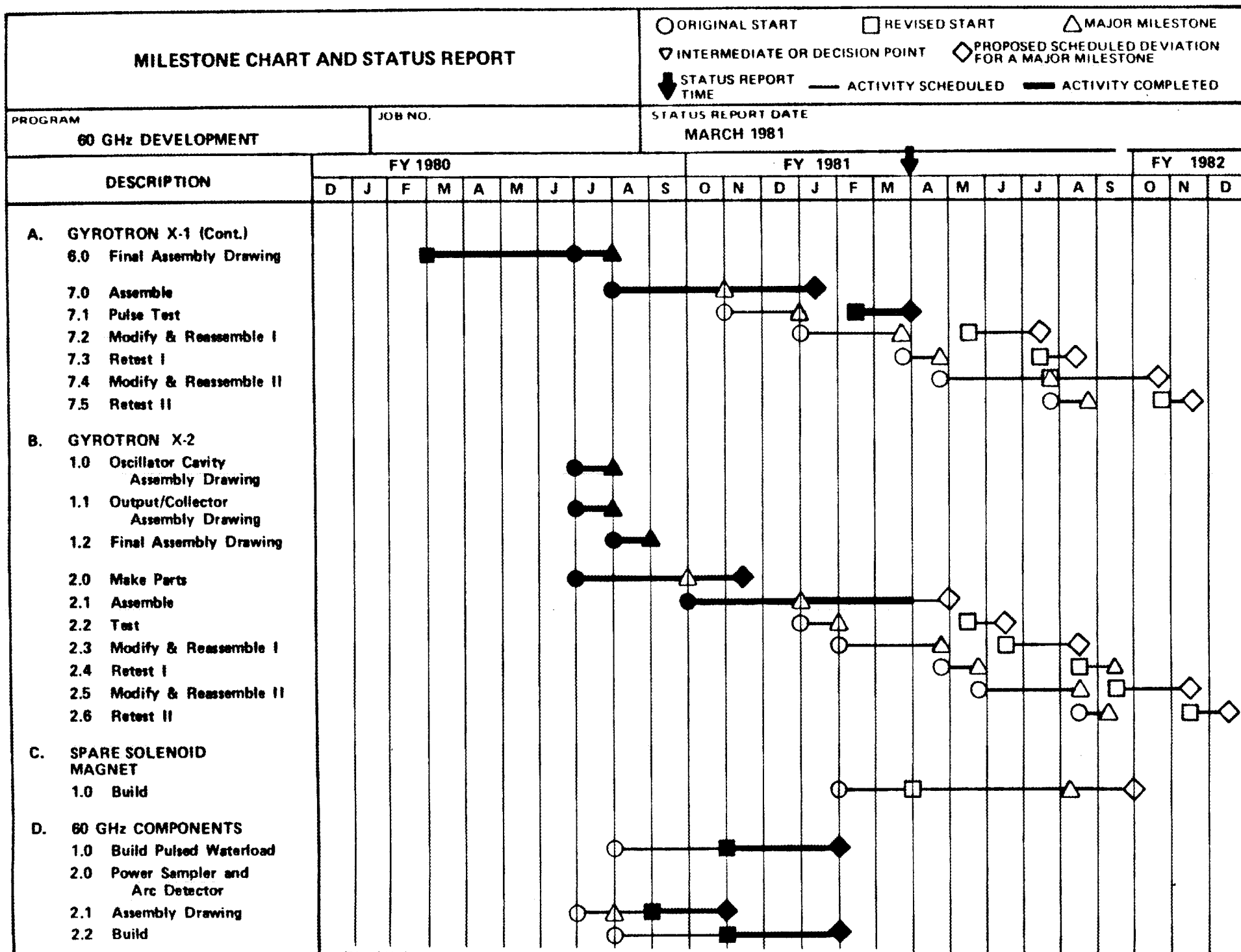


FIGURE 13. MILESTONE CHART AND STATUS REPORT (Cont.)

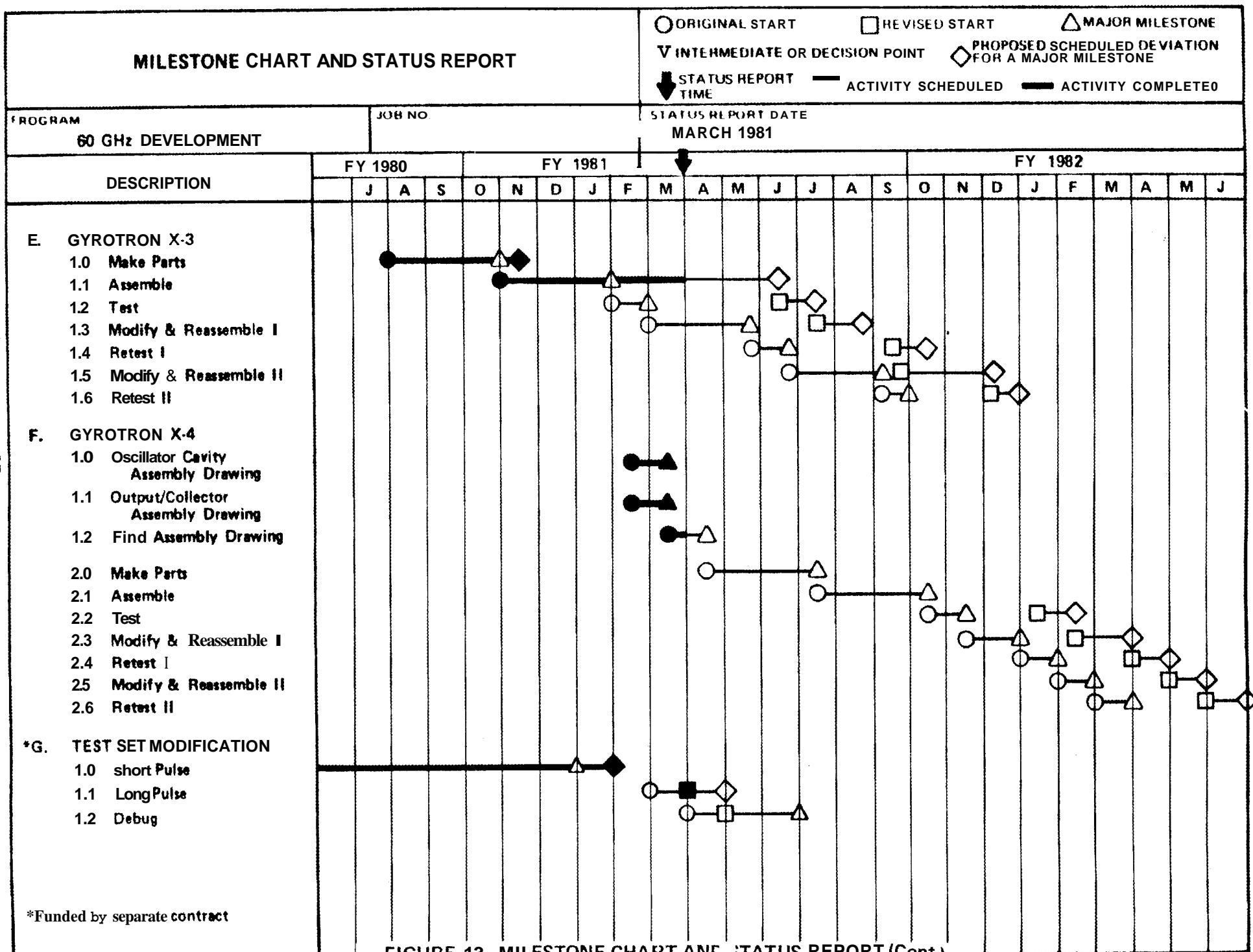
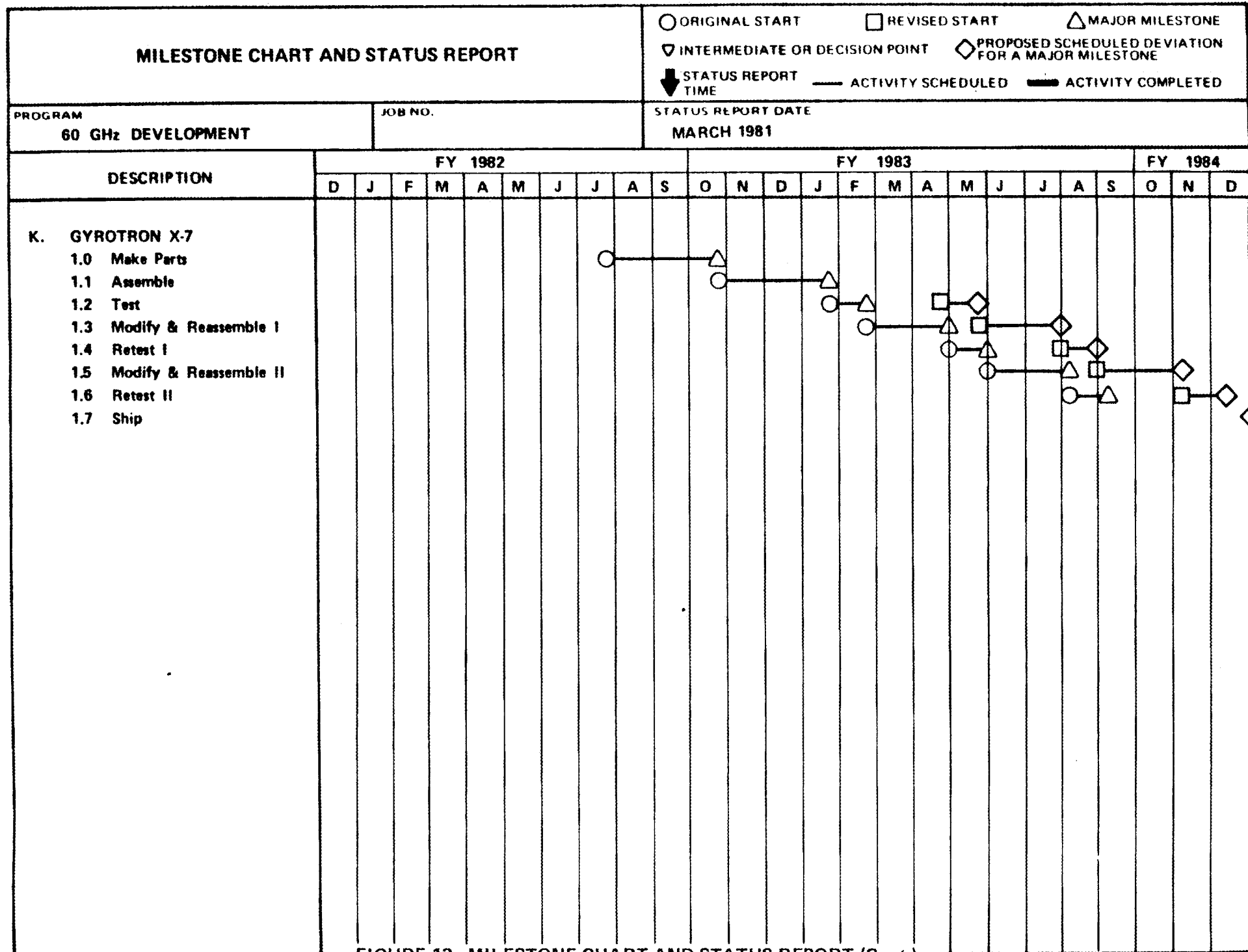
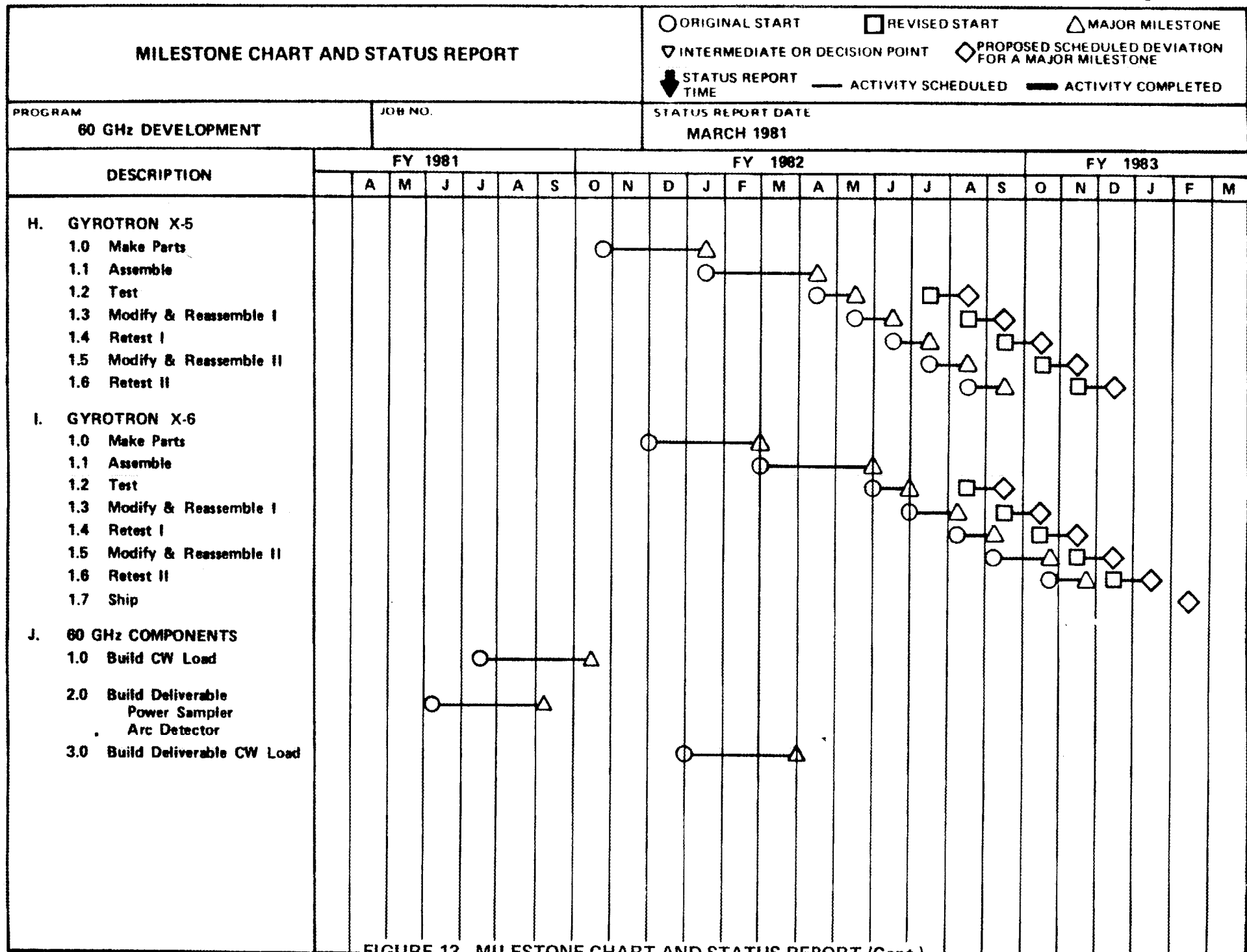
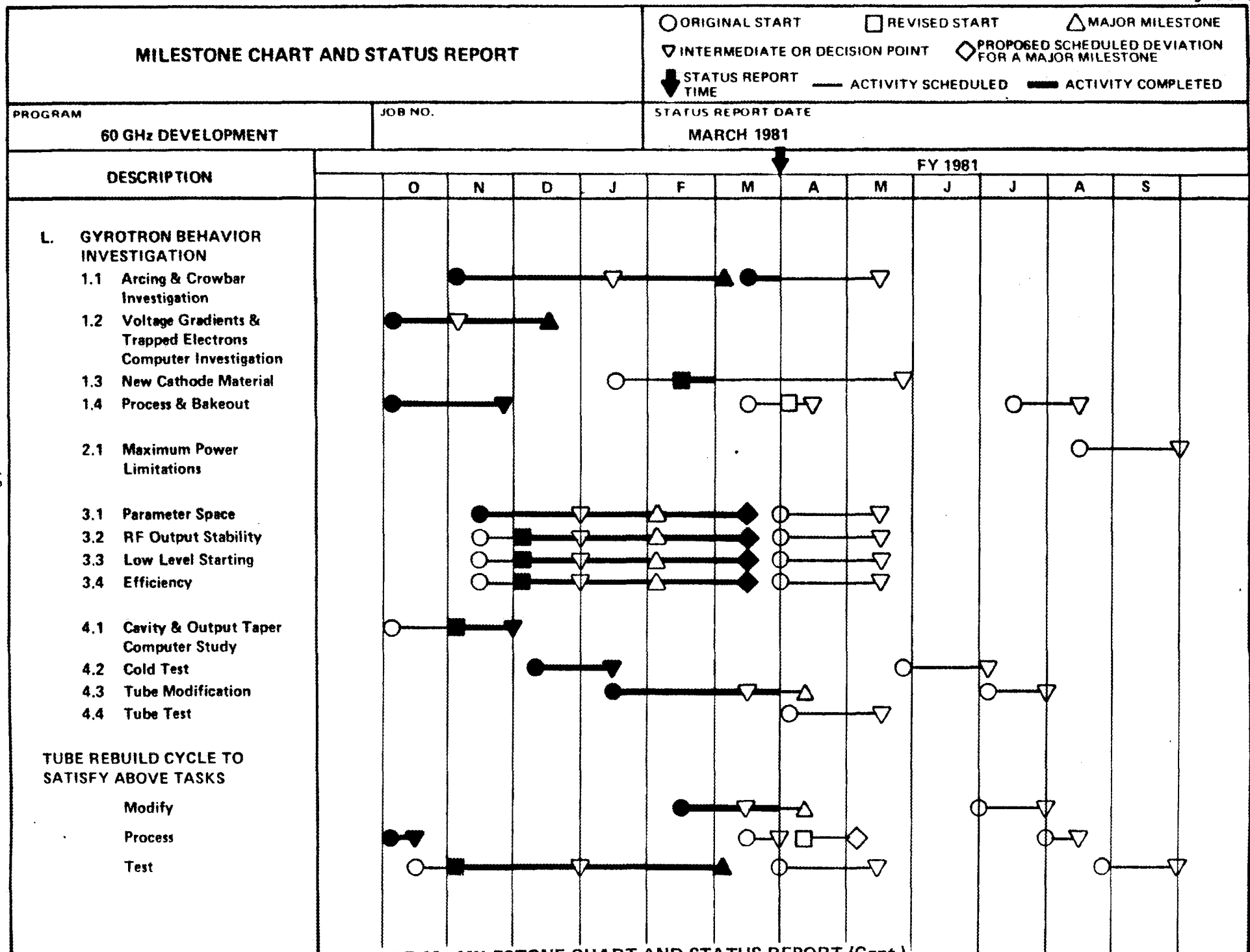


FIGURE 13. MILESTONE CHART AND STATUS REPORT (Cont.)







## X. REFERENCES

1. H. R. Jory, E. L. Lien, and R. S. Symons, Final Report, "Millimeter Wave Study Program", Oak Ridge National Laboratory Order No. Y12 11Y-49438 V, Varian Associates, Inc., November 1975.
2. D. V. Kisel, G. S. Korablev, V. G. Navel'yev, M. I. Petelin and Sh. E. Tsimring, "An Experimental Study of a Gyrotron, Operating at the Second Harmonic of the Cyclotron Frequency, with Optimized Distribution of the High Frequency Field," Radio Engineering and Electronic Physics, Vol. 19, No. 4, 95-100, 1974.
3. S. Hegji, H. Jory and J. Shively, "Development Program for a 200 kW CW, 28 GHz Gyroklystron" Quarterly Report No. 6, Union Carbide Corporation Contract No. 53X01617C, Varian Associates, Inc., July through September 1977.
4. H. Jory, S. Evans, S. Hegji, J. Shively, R. Symons and N. Taylor "Development Program for a 200 kW, CW, 28 GHz Gyroklystron", Quarterly Report No. 9, Union Carbide Corporation Contract No. W-7405-eng-26, ORNL Sub-01617/9, Varian Associates, Inc., April through June 1978.
5. V. A. Flyagin, et al, "The Gyrotron", IEEE Trans. MTT-25, No. 6 pp. 522-527, June 1977.
6. J. F. Shively et al, "Recent Advances in Gyrotrons," 1980 IEEE MTT-S International Microwave Symposium Digest, 28-30 May 1980, Washington, D.C. IEEE Catalog No. 80CH1545-3 MTT, pp 99-101.
7. F. Friedlander, E. Galli, H. Jory, F. Kinney, K. Miller, J. Shively and R. Symons, "Development Program for a 200 kW, CW 28 GHz Gyroklystron", Quarterly Report No. 1, Union Carbide Corporation Contract No. 53X01617C, Varian Associates, Inc., October 1976.
8. F. Friedlander, E. Galli, H. Jory, K. Miller, J. Shively, and R. Symons, "Development Program for a 200 kW, CW, 28 GHz Gyroklystron," Quarterly Report No. 2, Union Carbide Corporation Contract No. 53X01617C, Varian Associates, Inc. October 1976.
9. J. F. Shively, M. K. Cheng, S. J. Evans, T. J. Grant and D. S. Stone, "60 GHz Gyrotron Development Program", Quarterly Report No. 6, Union Carbide Corporation Contract No. 53Y-21453C, Varian Associates, Inc.
10. K. R. Chu, Phys. Fluids 21, 2354 (1978).
11. G. S. Nusinovich and R. E. Erm, Elektronnaya Tekhnika, Series 1, Elektronika UHF 1972, No. 8, pp 55-60.

ORNL/SUB-76/01617/  
June 16, 1981

INTERNAL DISTRIBUTION

1. A. L. Boch
2. J. L. Burke
3. R. J. Colchin
- 4-7. H. O. Eason
8. D. C. Eldridge
9. R. P. Jernigan
- 10-12. C. M. Loring
13. H. C. McCurdy
14. D. B. Morgan, Jr.
15. T. L. White
- 16-17. Laboratory Records Department
18. Laboratory Records, ORNL-RC
19. Y-12 Document Reference Section
- 20-21. Central Research Library
22. Fusion Energy Division Library
23. Fusion Energy Division Communications Center
24. ORNL Patent Office

EXTERNAL DISTRIBUTION

25. R. A. Dandl, 1122 Calle De Los Serranos, San Marcos, CA 92069
26. R. J. DeBellis, McDonnell Douglas Astronautics Co., P.O. Box 516, St. Louis, MO 63166
27. W. P. Ernst, Princeton University, Plasma Physics Laboratory, P.O. Box 451, Princeton, NJ 08540
28. W. Friz, AFAL/DHM, Wright Patterson AFB, OH 45433
29. T. Godlove, Particle Beam Program, Office of Inertial Fusion, Department of Energy, Mail Stop C-404, Washington, DC 20545
30. V. L. Granatstein, Naval Research Laboratory, Code 6740, Washington, DC 20375
31. G. M. Haas, Component Development Branch, Office of Fusion Energy (ETM), Department of Energy, Mail Stop G-234, Washington, DC 20545
32. G. W. Hamilton, Reactor Design, MFE Program, Lawrence Livermore National Laboratory, L6-44, P.O. Box 5511, Livermore, CA 94550
33. J. L. Hirshfield, Yale University, Department of Engineering and Applied Science, P.O. Box 2159, Yale Station, New Haven, CT 06520
34. J. V. Lebacqz, Stanford Linear Accelerator Center, P.O. Box 4349, Stanford, CA 94305
35. W. Lindquist, Electronics Engineering Department, Lawrence Livermore Laboratory, P.O. Box 808/L-443, Livermore, CA 94550
36. K. G. Moses, TRW Defense & Space Systems, 1 Space Park, Bldg. R-1, Redondo Beach, CA 90278
37. M. R. Murphy, Office of Fusion Energy (ETM), Department of Energy, Mail Stop G-234, Washington, DC 20545
38. J. H. Pfannmuller, McDonnell Douglas Astronautics Co., c/o Oak Ridge National Laboratory, P.O. Box Y, Bldg. 9983-32, Oak Ridge, TN 37830
39. G. F. Pierce, 53 Lamond Drive, Inverness, IL 60067
40. B. H. Quon, TRW Defense & Space Systems, 1 Space Park, Bldg. R-1, Redondo Beach, CA 90278
41. M. E. Read, Naval Research Laboratory, Code 6740, Washington, DC 20375
42. D. B. Remsen, General Atomic Company, P.O. Box 81608, San Diego, CA 92138
43. G. Simonis, Harry Diamond Laboratory, 2800 Powder Mill Road, Adelphi, MD 20783
44. B. Stallard, Lawrence Livermore Laboratory, University of California, L-437, P.O. Box 808, Livermore, CA 94550
45. H. S. Staten, Office of Fusion Energy (ETM), Department of Energy, Mail Stop G-234, Washington, DC 20545

ORNL/SUB-76/01617/  
June 16, 1981

- 46. P. T. Tallarico, AT-1, Accelerator Technology Division, Los Alamos Scientific Laboratory,  
Mail Stop 817, P.O. Box 1663, Los Alamos, NM 87545
- 47. J. J. Tancredi, Hughes Aircraft Company, Electron Dynamics Division, 3100 W. Lomita Blvd.,  
Torrence, CA 90509
- 48. R. J. Temkin, National Magnet Laboratory, Massachusetts Institute of Technology, Cambridge,  
MA 02139
- 49. A. Trivelpiece, Science Applications, Inc., 1200 Prospect Street, P.O. Box 2351, LaJolla,  
CA 92038
- 50. Director, U.S. Army Ballistic Missle Defense Advance Technology Center, Attn.: D. Schenk,  
ATC-R, P.O. Box 1500, Huntsville, AL 35807
- 51-52. Department of Energy Technical Information Center, Oak Ridge, TN 37830
- 53. RADC/OCTP, Griffiss AFB, NY 13441
- 54. Office of Assistant Manager for Energy Research and Development, Oak Ridge Operations Office,  
Department of Energy, Oak Ridge, TN 37830

U

VARIAN DISTRIBUTION

- 55. R. Berry
- 56. S. Evans
- 57. S. Evers
- 58. K. Felch
- 59. P. Ferguson
- 60. G. Huffman
- 61. G. Jacobson
- 62. H. Jory
- 63. J. Manca
- 64. J. Moran
- 65-68. J.F. Shively
- 69. S. Spang
- 70. A. Staprans
- 71. D. Stone
- 72. R. Symons
- 73-75. R.M. West